Spatial variation in the joint effect of extreme heat events and ozone on respiratory hospitalizations in California

Lara Schwarz[a,b,1,2], Kristen Hansen[b,1,2], Anna Alari[c], Sindana D. Ilango[d], Nelson Bernal[e], Rupa Basu[f], Alexander Gershunov[g], and Tarik Benmarhnia[b,g]

[a]School of Public Health, San Diego State University, San Diego, CA 92182; [b]Herbert Wertheim School of Public Health and Human Longevity Science, University of California San Diego, La Jolla, CA 92093; [c]Sorbonne Université, INSERM, Institut Pierre Louis d'Épidémiologie et de Santé Publique, NEMESIS (Neighborhood Environments and Mobility: Effects on Social health InequalitieS) Research Team, F75012, Paris, France; [d]Department of Epidemiology, University of Washington, Seattle, WA 98195; [e]Center for Sustainable Development, University of Brasilia, Brasilia 70910-900, Brazil; [f]Office of Environmental Health Hazard Assessment, California Environmental Protection Agency, Oakland, CA 94612; and [g]Scripps Institution of Oceanography, University of California San Diego, La Jolla, CA 92038

Edited by Douglas S. Massey, Princeton University, Princeton, NJ, and approved April 11, 2021 (received for review November 8, 2020)

Extreme heat and ozone are co-occurring exposures that independently and synergistically increase the risk of respiratory disease. To our knowledge, no joint warning systems consider both risks; understanding their interactive effect can warrant use of comprehensive warning systems to reduce their burden. We examined heterogeneity in joint effects (on the additive scale) between heat and ozone at small geographical scales. A within-community matched design with a Bayesian hierarchical model was applied to study this association at the zip code level. Spatially varying relative risks due to interaction (RERI) were quantified to consider joint effects. Determinants of the spatial variability of effects were assessed using a random effects metaregression to consider the role of demographic/neighborhood characteristics that are known effect modifiers. A total of 817,354 unscheduled respiratory hospitalizations occurred in California from 2004 to 2013 in the May to September period. RERIs revealed no additive interaction when considering overall joint effects. However, when considering the zip code level, certain areas observed strong joint effects. A lower median income, higher percentage of unemployed residents, and exposure to other air pollutants within a zip code drove stronger joint effects; a higher percentage of commuters who walk/bicycle, a marker for neighborhood wealth, showed decreased effects. Results indicate the importance of going beyond average measures to consider spatial variation in the health burden of these exposures and predictors of joint effects. This information can be used to inform early warning systems that consider both heat and ozone to protect populations from these deleterious effects in identified areas.

extreme heat | ozone | health | joint effects | spatial analysis

Early warning systems for air pollution (1, 2) and heat (3, 4) have been implemented in various areas to limit the health impact of these increasingly prevalent environmental stressors (5, 6). Extreme heat events and some air pollutants such as tropospheric ozone have similar meteorological drivers, as they result from chemical reactions between volatile organic compounds, nitrogen oxides (NOx), and sunlight, leading them to regularly coincide (7). However, no joint early warning systems have been implemented to combat the dual burden of these environmental health risks. An improved understanding of these risks and the interaction between these hazards is important to inform the development and use of early warning systems that consider these joint exposures.

The adverse health effects of heat are well documented. For example, exposure to high ambient temperature has been shown to increase the risk of mortality and morbidity for a range of diseases (8, 9). High ambient temperature causes heat stress and decreases ability to thermoregulate efficiently, which can produce heat-related inflammation and cardiac stress (10). Several studies have found impacts of heat on respiratory hospital admissions, such as chronic obstructive pulmonary disease and an increase in respiratory infections leading to increased hospitalizations (11–14).

Ozone is a reactive, oxidative gas that is absorbed by the upper respiratory tract; epidemiological studies show a robust relationship between acute exposure to ambient ozone and morbidity (15). Ozone pollution is associated with a range of adverse health effects induced by oxidative stress and increased risk of respiratory disease, such as acute respiratory illnesses and asthma (15–18). In 2015, it was reported that globally, 4.1 million disability-adjusted life years were attributable to ozone exposure alone (19).

Ambient ozone increases under high ambient temperature and blazing sunlight, both of which are characteristics of extreme heat events (15). Due to the comparable meteorological patterns, heat and ozone are co-occurring risk factors, and a number of studies have considered the potential concurrent risks and interaction of these exposures in driving the health burden (20–22). Studies in Brisbane, Australia, and in the Netherlands suggested that both ozone and heat play a role in increasing

Significance

Projections show that extreme heat events and high ozone days are expected to increase under climate change. Both exposures are harmful to human health, but warning systems, typically implemented separately, do not consider the joint effects of these exposures. In this study, we propose a method to address spatial differences of the joint effects of extreme heat events and ozone peaks on respiratory hospitalizations at the zip code level in California. Zip codes with low median income and high unemployment rates are at increased risk for these joint effects. Results identified zip codes with increased vulnerability, demonstrating the importance of going beyond average measures to prioritize areas for joint warning systems and protect population health.

Author contributions: L.S., K.H., R.B., and T.B. designed research; L.S., K.H., S.D.I., N.B., and T.B. performed research; L.S., K.H., and S.D.I. analyzed data; and L.S., K.H., A.A., S.D.I., N.B., R.B., A.G., and T.B. wrote the paper.

The authors declare no competing interest.

This article is a PNAS Direct Submission.

[1]L.S. and K.H. contributed equally to this work.

[2]To whom correspondence may be addressed. Email: lnschwar@health.ucsd.edu or k1hansen@health.ucsd.edu.

This article contains supporting information online at https://www.pnas.org/lookup/suppl/doi:10.1073/pnas.2023078118/-/DCSupplemental.

Published May 24, 2021.

excess deaths during a heat wave (23, 24). Interaction between both exposures suggests that the effect of both ozone and heat drive an increased burden compared to each exposure individually. Findings differ between these studies, some revealing a strong relative interaction (20, 25, 26), while others demonstrate a weaker signal (27, 28) or no joint effect (29). For example, high temperature enhanced the effects of ozone on all-cause mortality in France (20) and cardiovascular and respiratory deaths in China (22). In contrast, no relative interaction between ozone and heat was observed in all but one city in England (23).

Although several studies have considered the joint effects of temperature and ozone (20, 26, 27), few have considered the fine spatial variation in these effects (30). The consideration of fine spatial variation is important because it can provide location-specific thresholds that are most effective in revealing this health burden. Studying spatial variation across diverse regions is vital because it can reveal the heterogeneity of this interaction that can be used to inform warning systems. One study applied a spatial semiparametric model to estimate the joint effects of ozone and temperature risk in urban areas in the United States (30). Although that paper finds evidence of ozone–temperature interaction at high temperature thresholds and ozone concentrations, the study focused on urban areas and the relationship varied by city studied. Therefore, we were motivated to consider this interaction at the zip code level in various geographical and sociodemographic contexts.

Some vulnerable groups are known to be especially susceptible to the effects of ozone and heat. For example, the ozone-related excess attributable risk was found to be almost two times higher for Black compared to White residents in California for air pollution exposure above federal standards (31). Racial discrimination plays a role, as decreased access to primary care, private insurance, and preventive medication of Black residents when compared to their White counterparts likely drive this health disparity (31). Furthermore, racial minorities and communities of a low socioeconomic status are also more susceptible to heat-related health effects; this is associated with poorer physical health, lower access to air conditioning, and greater neighborhood-level exposure that may increase risk (32). Green space, for example, has been shown to be a modifier of heat-related health effects (14). Although these contextual variables are known to play a role in the effect of these exposures, no study to our knowledge has considered the role of sociodemographics and neighborhood-level factors in driving the interactive effect between ozone and heat.

We examined the potential heterogeneity in the joint effects between heat and ozone resolving fine geographical scales. The majority of studies considering joint effects have not used heat waves or extreme heat events as a binary variable to study temperature effects. We argue that studying the effects of temperature exceeding thresholds is a policy-relevant measure that can be used to activate early warning systems (9). Moreover, most studies focus on mortality, and very few have considered the burden on hospitalizations, a more moderate signal that could reveal broader health impacts. Lastly, the majority of studies investigated heat–ozone interactions based on the relative scale by including a product term in multiplicative models (33, 34). In this study, we investigate interaction on the additive scale that constitutes a more relevant public health measure (35, 36) since it directly quantifies the absolute number of hospital admission cases that could be prevented by a joint intervention on both heat and ozone exposures as compared to independent interventions. Focusing on the highly diverse state of California, we explore the role of sociodemographics and environment characteristics at the zip code level in predicting these joint effects to identify factors that can be used to prioritize areas for joint warning systems.

Materials and Methods

Data Sources.

Environmental data. Temperature data from the National Oceanic and Atmospheric Administration's vast Cooperative Observer and First Order stations were used for this study (37). The minimum and maximum daily temperature (°C) observations at these stations spanning 1950 through 2013 had been interpolated onto a 1/16° (~6 km) grid (38). Population-weighted centroids for each Zip Code Tabulation Area (ZCTA) were linked with the nearest temperature measurements using the *geonear* function in Stata15 SE. The distance from each centroid to a temperature grid cell center therefore did not exceed 6 km. Unpopulated areas such as national parks are excluded from the ZCTA delineations, so no data are provided for these areas.

Various extreme heat events were defined when the daily maximum or minimum temperature exceeded the 99th, 97.5th, or 95th percentile of the temperature distribution for each ZCTA for 1 d and 2 consecutive days during the warm season of May to September. We considered a total of six extreme heat event definitions during the warm period (Table 1). Each of these definitions were examined using maximum and minimum temperature to consider daytime- and nighttime-accentuated extreme heat events, as nighttime-accentuated heat typically occurs in anomalously humid conditions (39), which hold special health risks.

Ozone data were estimated at the daily level using 8-h maximums sampled and analyzed by the US Environmental Protection Agency (EPA) Air Quality System (40). Measured concentrations from fixed-site monitoring stations within a 20 km radius of each population-weighted zip code centroid were used for interpolation (reference *SI Appendix*, Fig. S9 for the spatial distribution of ozone estimates missingness). To capture acute exposure to high ozone levels, five definitions of ozone peaks were estimated at various percentiles of the ozone distribution for each ZCTA. The 99th, 95th, 90th, and 75th percentiles of the May through September period were considered as well as a standard threshold of 70 parts per billion (ppb), which corresponds to the EPA National Ambient Air Quality Standard for ozone (41).

Hospitalization data. Unscheduled hospitalizations in California from 2004 through 2013 were obtained from the Office of Statewide Health Planning and Development Patient Discharge Data. This included all hospital visits that were not prearranged, including emergency department visits and hospital admissions; these together will be referred to as hospital visits in the remainder of this manuscript. Variables of interest included ZCTA of the patient's residence, day of the week, and hospitalization outcome, which was aggregated into daily counts for each ZCTA in California. Respiratory disease (International Classification of Diseases Ninth Revision code: 460–519) hospital visits were considered as the outcome of interest due to the well-documented association with both ozone and extreme heat.

Statistical Analysis.

Case-crossover methodology for the California overall effect. A time-stratified case-crossover design was used to study the association between each extreme heat event definition, ozone peak, and hospital visits for respiratory disease (42–44) to understand average joint effects in California as a whole. Controls were identified for each case in the study population and selected based on the same day of the week of the hospital visit within the same month and year that the case occurred. Only time-varying variables were considered as covariates in models. A RERI was then calculated to consider the overall joint effect of ozone and extreme heat events for California (36). We first assessed the average joint effect of ozone and extreme heat across the entire state.

Within-community matched design analysis. A within-community matched design was then used to study the association between extreme heat events and ozone exposure and hospital visits for respiratory disease at the zip code level to further understand whether spatial variation played a role in average overall effect. This approach offers benefits over previous approaches by allowing the investigation of interactive effects at the zip code level. For each exposed day, we identified all possible controls based on two criteria: 1) matches must be in the same zip code, and 2) matches must be in the same summer. We used an inverse time weighting scheme to calculate the comparison averages of hospitalizations on those control days for the contrast. For example, control days closer in time to the exposed day were given a stronger weight than those that were further in time. A RERI was calculated for each ZCTA to consider the joint effects of ozone and extreme heat events at the zip code level (45, 46). Three relative risks (RRs) were computed for each zip code using the control day weighted averages mentioned above where we compared rates in joint extreme heat events (HW)/O_3 days RR_{11} (RR_{joint}), HW only RR_{10}(RR_{hw}), and O_3 only RR_{01}(RR_{ozone}) days to days without any HW nor O_3 event RR_{00} ($RR_{neither}$), where HW is the extreme heat event and O_3 is ozone. For each independent occurrence of an ozone peak and an

Table 1. Characteristics of respiratory hospital visits and summary of daily temperature and ozone pollution in California, May to September 2004 to 2013

Health outcome	*n*	Mean daily cases (SD)
Respiratory hospital visits	817,354	677 (195)
Environmental exposures	**Threshold**	**No. ZCTA days exceeding threshold for 2,863 ZCTAs**
Heat waves (°C)	Mean ± SD	
Maximum temperature		
97.5th 1 d	37.75 ± 4.11	69,692
99th 1 d	38.95 ± 3.85	28,616
97.5th 2 d	38.37 ± 3.98	34,612
99th 2 d	39.57 ± 3.78	11,391
Minimum temperature		
97.5th 1 d	20.29 ± 4.21	69,783
99th 1 d	21.27 ± 4.22	28,679
97.5th 2 d	21.08 ± 4.00	33,394
99th 2 d	22.10 ± 3.88	12,105
Ozone waves (ppb)		
99th	79.92 ± 15.36	23,126
95th	71.58 ± 15.00	110,122
90th	67.49 ± 14.87	217,272
75th	61.67 ± 14.41	534,519
70 ppb	78.07 ± 7.81	187,227

extreme heat event, we calculated RR by taking the total number of respiratory hospitalizations in a zip code on a case day versus the weighted average on all control days for that particular case day (extreme heat event, ozone peak), and then similarly RRs for the joint heat and ozone days were calculated. When all RRs were calculated for a zip code, we used the average to produce zip code–level RR estimates. Thus, RERI was calculated by the following equation:

$$RERI = (RR_{joint} - 1) - (RR_{HW\overline{ozone}} - 1) - (RR_{ozone\overline{HW}} - 1).$$

This quantifies the joint effects at this fine spatial domain on the additive scale (45). The within-community matched design focused on extreme heat events using the 95th percentile of maximum temperature and ozone peaks at the 75th percentile to capture sufficient joint-effect days for analysis.

With an outcome of interest such as hospital visits, we expect there to be many days in low population zip codes where there are zero hospital visits. For this reason, some of the RRs are very small for small population zip codes on case days. Due to the weighted average being used as a denominator for our RRs, we do not encounter many zeros in the denominator. The few case days where there was a zero-value denominator, the numerator was also zero. Thus, the scarcity of data did not pose a significant problem for our analysis; however, for the smallest population zip codes, we do not observe precise estimates. Incorporating information from surrounding zip codes can improve precision, and thus, a spatial analysis is beneficial.

Analyses were conducted on Stata 15/SE and R. For reproducibility purposes, a coauthor that was not involved in the analysis reviewed the code for the study. Additionally, the code and a sample dataset for reproducibility purposes is provided at the following link: https://github.com/benmarhnia-lab/JointOzoneHeatWaves.

Bayesian hierarchical model extension. We expect there to be spatial autocorrelation in our RERI estimates. Due to data scarcity, leveraging this spatial information can increase the precision in our estimates. Similarly to Aguilera et al. we used a spatial Bayesian hierarchical model (BHM) for this purpose (47). BHMs provide a decrease in variance of estimates by using information spatially near any point. The RERI estimates for each zip code obtained from the within-community matched design analysis were used as the response variable in a spatial linear model. The Bayesian model was fit using the spBayes package in R (48). This package requires the use of point-referenced data rather than areal regions, and for this we used population-weighted centroids from the US Census Bureau (49). We fit an empirical semivariogram to estimate the starting values for the spatial parameters: sill (σ^2), nugget (τ^2), and range (ϕ). Based on the shape of the semivariogram, a spherical covariance structure fit the most closely to the data. The spherical covariance function is commonly used in spatial analyses and has the following form:

$$C_{sph}(h) = \begin{cases} \sigma^2\left(1 - \frac{3}{2}\frac{|h|}{\phi} + \frac{1}{2}\frac{|h|^3}{\phi^3}\right), 0 \le |h| \le \phi \\ 0, |h| > \phi \end{cases}.$$

The covariance structure is specified in the model implementation, which forces the covariance matrix to hold this form. All covariance structures for this type of model are isotropic.

The model forms a hierarchical model with two stages:

the first stage is $Y|\theta, Z \sim N(X\beta + Z, \tau^2 I)$, and

the second stage is $Z|\sigma^2, \phi \sim N(0, \sigma^2 H)$,

where θ is the vector of parameters including β, sill, nugget, and range, and Z is the vector of spatial random effects. Conditionally, $Y_i|Z$ are independent. H represents the spatial correlation structure, which we set as spherical in this case. The second stage model, called the process model, is introduced to capture spatial dependence in the outcome variable. Model specification finally includes adding starting, tuning, and distribution values for our priors of parameters τ^2 and the hyper parameters ϕ and σ^2. The model captures the spatial process underlying the distribution of RERI in California from 2004 through 2013. This model generally can be considered a spatial Bayesian extension to a general linear model.

The prior distributions and tuning parameters we used allowed for minimal impact on the final values. Monte Carlo Markov chain samples are used to estimate parameters. We used 10,000 samples, 75% for burn-in. An 800 × 800 raster grid was produced by interpolating the recovered sample weights using multilevel B-splines. This methodology assumes isotropy, although that may not hold in the case of environmental variables.

To represent the precision of the point estimates, we computed the signal-to-noise ratio (SNR) from the model output, which includes weight and SEs. The SNR was mapped for each ZCTA to represent statistical precision. This gives a visual representation of areas where estimates of RERI from the BHM are precise. We use the traditional cutoff when |SNR| > 2 to represent precision. Additionally, as acclimation and adaptation can modify the effects of heat (50) and ozone (51), respectively, a sensitivity analysis was conducted considering stratified estimates for each month of study, to consider the potential differing effect of these exposures throughout the summer.

Metaregression. Once spatial estimates from the BHM were output, we used them in a metaregression to understand the factors influencing these joint effects of ozone and heat over space. Demographic and environmental variables were retrieved from the US Census American Community Survey (49) and the Healthy Places Index (52). The variables we considered for this analysis were neighborhood and demographic variables that have been shown to be related to ozone and heat effects. These include population density, the percentage of residents that are non-White, Black, over 65 y of

age, female, unemployed, without health insurance, foreign born, and race and environmental variables such as the percentage of the zip code with tree canopy, access to parks, and concentrations of other pollutants ($PM_{2.5}$, PM_{10}, NO_2). We additionally included variables about lifestyle, including accessibility of parks, the percentage of commuters who walk or ride a bike, and automobile ownership. The normalized difference vegetation index (NDVI) was used to characterize green space at the zip code level. Finally, we create a composite score from the eigenvectors of the first principal component derived from the principal component analysis (PCA); we use this composite score as another variable. Each variable was considered in a univariate linear model, with the spatial estimates output from the BHM as the outcome. Effect estimates and CIs were taken from each model to represent the significance of each variable in the spatial distribution of joint ozone and heat effects.

Results

Study Population and Summary of Exposures. A total of 817,354 unscheduled respiratory hospitalizations occurred from 2004 to 2013 in 543 hospitals (map shown in *SI Appendix*, Fig. S8) in California (Table 1). Temperature and ozone thresholds for various extreme heat event and ozone peak definitions are also described in Table 1. For example, extreme heat events defined by the 99th percentile using maximum temperature across all ZCTAs have an average threshold of 38.95 °C, ranging from 22.5 °C at the coast of Northern California to 49.8 °C in the southern desert, and a total of 28,616 ZCTA days are considered extreme heat event days using this definition (Table 1). There is coherent spatial variation in what temperature value corresponds to specific percentiles throughout California; the variation in the maximum temperature threshold is shown for the 95th percentile of the temperature distribution in Fig. 1, ranging between 20 °C in the coastal redwood forest of Humboldt County in far Northern California as well as in the high southern Sierra Nevada mountains to greater than 45 °C in the Mojave and Colorado/Sonoran Deserts in the far southeast. For ozone peaks, whose spatial distribution largely reflects that of temperature but locally modified by the distribution of population centers and industrial activity around the state, the overall average concentration is 79.9 ppb with an SD of 15.3 for the 99th percentile definition; 23,126 ZCTA days fall within these concentration levels (Table 1). In subsequent results, ozone peaks were considered at the 75th percentile to ensure sufficient ozone days could be analyzed.

Isolated Effects of Extreme Heat Events and Ozone Exposures. Fig. 2 shows the association between extreme heat events and ozone peaks separately and respiratory hospital visits for California. Extreme heat events defined using maximum temperature revealed greater health impacts than extreme heat events defined using minimum temperature (Fig. 2). Therefore, maximum temperature extreme heat events were emphasized in the following analyses. Overall, the majority of thresholds used for ozone peaks appear to be associated with increased hospital visits (Fig. 2). Overall, results showed that ozone and extreme heat events were independently associated with respiratory disease hospital visits in some areas of California, but this association is not consistent.

Joint Effects and Spatial Variation. When considering average joint effect in all of California, the RERIs revealed no effect for any combination of extreme heat events and ozone peak definition (*SI Appendix*, Table S1). However, when considering spatial differences in effect at the zip code level within California, the variation is revealed (Fig. 3). Differences in RERI estimates considering extreme heat events at the 95th percentile and ozone at the 75th percentile within California demonstrated that some areas showed a strong joint effect with RERIs exceeding values of 2, and other areas indicate negative interaction of values lower than −2 (Fig. 3). Hotspots that show strong joint effects are sparse, peppering the state here and there. Examples of these hotspots include a spot along the United States–Mexico border area and a sizable area in the western Central Valley along the San Joaquin River. It is important to note that the high variation leads to imprecise estimates of joint effects through RERI; precision of estimates can be seen in *SI Appendix*, Figs. S1 and S2. The results of spatial heterogeneity in RERI when the ozone peak is defined by an absolute threshold of 70 ppb are shown in *SI Appendix*, Figs. S3 and S4. However, some information is missing for this definition because of many ZCTAs never reaching 70 ppb for ozone. The definitions of both extreme heat events and ozone peaks analyzed showed distinct spatial differences.

We consider the lagged effect of these joint days by considering the average hospitalizations on the two following days after an event. *SI Appendix*, Fig. S5 displays the Bayesian surface of the RERI estimates. Overall, we find lower effect sizes but higher precision for this analysis. The sensitivity analysis considering stratified estimates for each month of study showed some variation in spatial patterns throughout the summer, indicating that acclimation may play a role in some ZCTAs (*SI Appendix*, Fig. S6). However, we did not identify a strong attenuation of effect, and acclimation does not seem to be a major driver of our observed results.

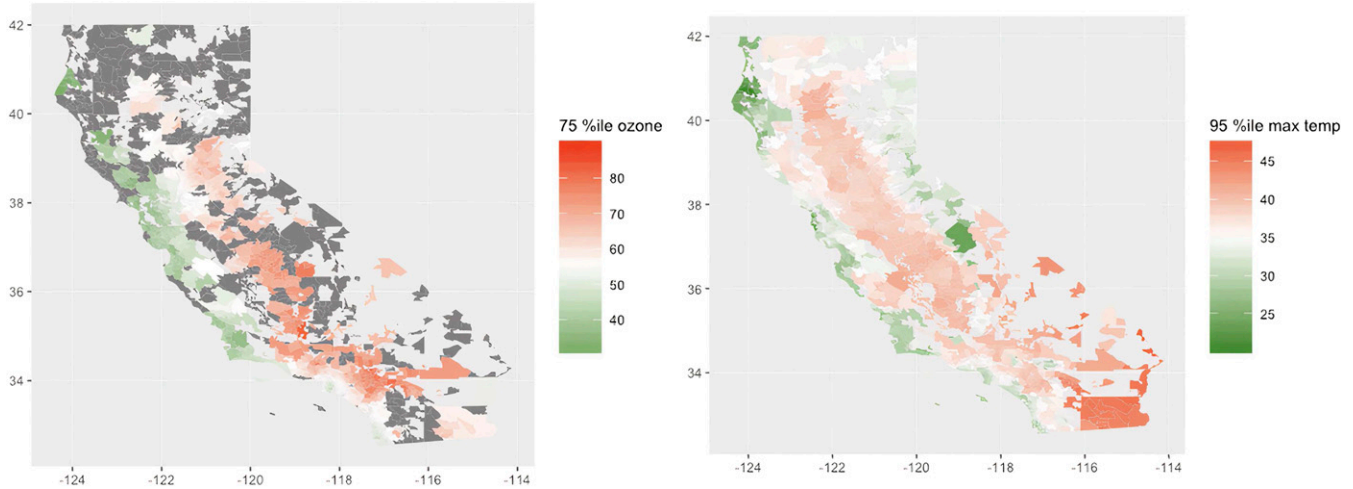

Fig. 1. Spatial distribution of exposure values that corresponds to a 75th percentile of ozone (ppb) and 95th percentile of maximum temperature (°C) during the warm season (May to September) for each ZCTA, 2004 to 2013 in California. Light gray areas indicate ZCTAs with no data, and gray areas indicate ZCTAs with no climate data.

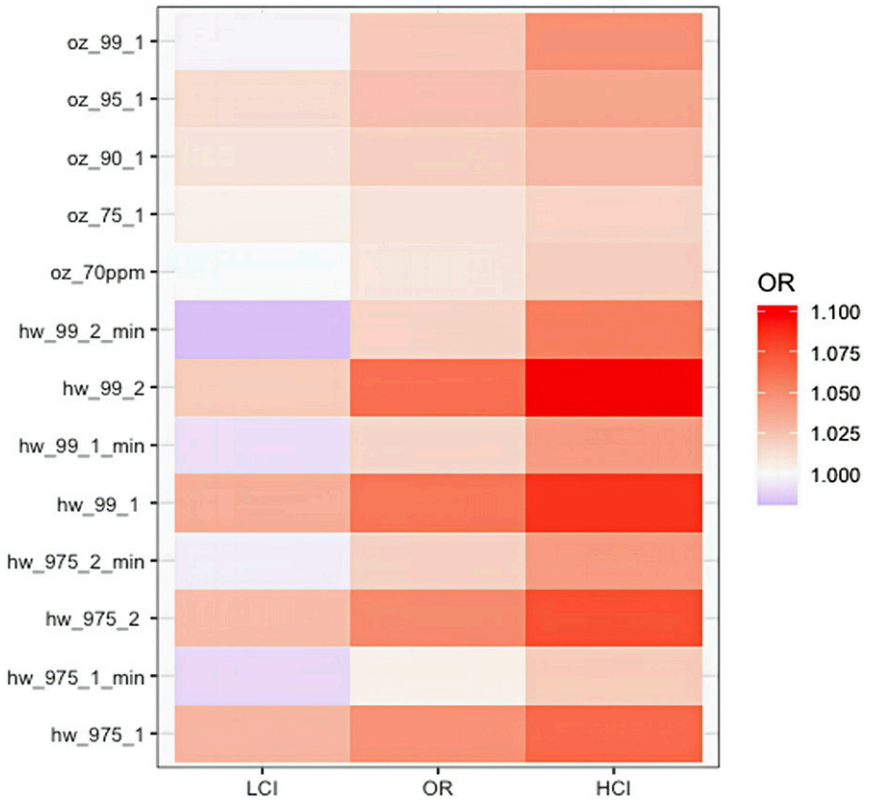

Fig. 2. Odds ratios and 95% CI of the bivariate association between heat waves (99th 1 d, 99th 1 d, 97.5th 1 d, and 97.5th 2 d), ozone peaks (99th, 95th, 90th, 75th, and 70 ppm), and respiratory hospital visits in California, 2004 to 2013.

Prediction of Joint Effects Using Neighborhood-Level Sociodemographics. Descriptors of variables included in the metaregression for all California zip codes are shown in *SI Appendix*, Table S3. Results of the metaregression showed that zip codes with a higher percentage of non-White residents, unemployed residents, and population with no health insurance were associated with stronger joint effects (Fig. 4). However, these variables are correlated with other demographic variables considered (*SI Appendix*, Fig. S7).

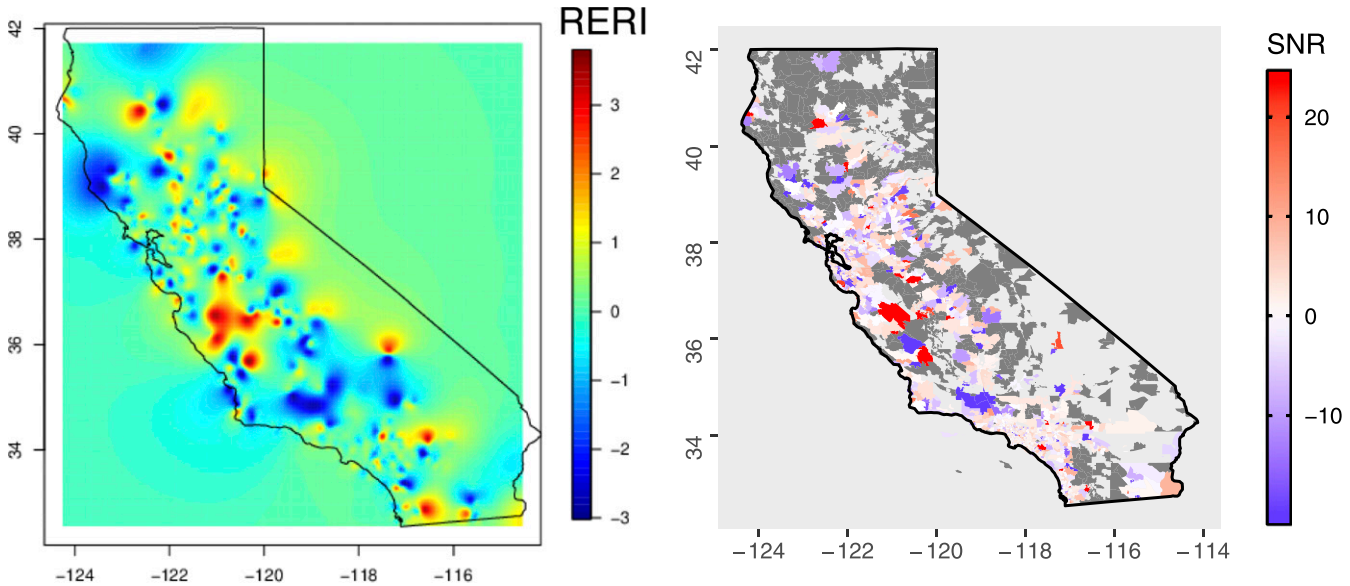

Fig. 3. Interpolated spatial distribution of joint effects of heat waves at the 95th percentile of maximum temperature (°C) and ozone peaks (ppb) at the 75th percentile on respiratory hospital visits using RERI in California, 2004 to 2013 from a BHM. (*Left*) The right displays the SNR (signal-to-noise ratio) for the BHM estimates, dark gray area indicates missing ozone data, red and blue indicate significance of a BHM estimate in a positive or negative direction, respectively. Light gray areas indicate no population and therefore no ZCTA.

After accounting for median income, an effect for the percentage of non-White residents is no longer observed (*SI Appendix*, Table S4) because of the high correlation between these two variables leading to a model that is less reliable for identifying effects. Zip codes with higher concentrations of other pollutants were also associated with stronger effects, while a higher percentage of commuters who walk or ride a bike was associated with decreased joint effects, although this effect was attenuated after adjusting for socioeconomic status (*SI Appendix*, Table S4). Park accessibility, tree canopy, the percentage of female residents, the percentage of residents with air conditioning, and those over 65 y of age showed imprecise predictions. The composite score produced from PCA showed high influence from the variables NDVI, no health insurance percentage, percent non-White, and mean NO_2. The PCA score was precise and relatively high in magnitude as we would expect.

Discussion

The results of this study indicate that the effects of ozone and heat are highly heterogeneous throughout California; some areas show strong joint effects, while other parts of the state suggest no interaction, or negative interaction, between ozone and heat. This validates the importance of considering the effects of these exposures at a local scale. Understanding which spatial units (e.g., ZCTA) have joint heat and ozone effects in a large geographically and demographically complex region such as California can inform warning systems and provide motive for considering thresholds of both ozone and heat exposures to activate these warning systems in specific geographical areas. More specifically, understanding how zip code–level demographic and environmental information is associated with these joint effects can be used to prioritize resources.

In California, the forecasting system includes extreme heat events; the National Weather Service uses an early warning system to identify potential heat risks at a local scale, which provides guidance to decisionmakers to take action (53). This resource forecasts potential threats of dangerous high heat year round but to our knowledge does not take into account the joint effects of ozone and heat. Our results highlight an opportunity to identify spatial heterogeneity to inform joint warning systems at this localized scale. Interestingly, no large-scale spatial pattern was observed, but "hotspots," such as the strongest positive joint effects, were observed in certain areas such as the Central Valley and the southern border region (Fig. 3). When considering a smaller scale, what appeared to be large-scale noise showed local signals at the ZCTA level. The results of the metaregression show that specific demographic and zip code–level information are drivers of these interactive effects. By identifying these areas that experience joint effects of ozone and heat, interventions considering thresholds of both exposures have the potential to prevent more cases of respiratory disease when implemented in addition to two independent interventions.

Heat warning systems have been shown to be effective at decreasing the deleterious effects of heat exposure (3, 54, 55). In particular, the thresholds of local heat emergency plans can be adapted based on evidence from epidemiological studies, which have been shown to increase the health benefits of activating heat action plans (54). Warning systems can be adapted to consider the joint effects of air pollutants such as ozone, which our results show would be beneficial in specific areas throughout California. This study and others considering fine spatial variation in the effect of environmental exposures can be valuable to define and target these specific regions.

A literature review was conducted for studies investigating the joint effect of ozone and heat on health (*SI Appendix*, Table S2).

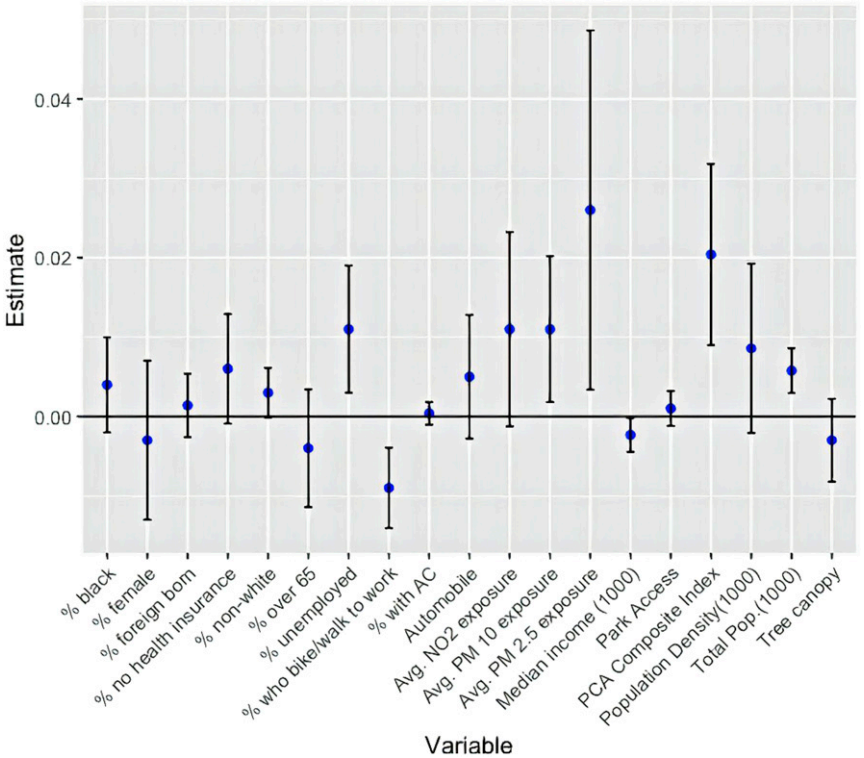

Fig. 4. Results of metaregression showing the association between standardized sociodemographic characteristics at the zip code level and joint effects of heat waves at the 95th percentile of maximum temperature (°C) and ozone peaks (ppb) at the 75th percentile on respiratory hospital visits in California, 2004 to 2013.

Most of the literature considering the joint effects of heat and ozone have presented assessments of average exposures in specific geographic areas such as cities or counties, primarily in Asia and Europe (28, 33, 34). Studies have found conflicting results, ranging from indications of strong interaction (56, 57) to no interaction (29). Another study found a negative association between ozone exposure and mortality on hot days (58). Two papers considering different cities or geographical areas found spatial variation in their results; Pattenden et al. found ozone–heat interaction in only one conurbation in England (London) out of the 15 studied (27). Similarly, Ren et al found synergistic associations in communities in the northeast but not in the southeast of the United States (25, 59).

Our results shed light on some of the variation in the findings of previous studies, some of which may be explained by differences in sociodemographics and environmental factors at the local level. Fig. 3 shows the spatial distribution of the effect of extreme heat events on respiratory hospital visits, which is highly heterogeneous (60, 61). When considering joint effects, the overall results for the entire state of California showed no interaction between ozone and extreme heat events (*SI Appendix*, Table S1). However, there is a wide spatial variation in the effects of heat, ozone, and the interaction of both as observed in Fig. 3. Some areas show negative interaction. There is evidence to suggest that reductions in NOx are associated with an increase in ozone concentrations (62); these ozone precursors, such as nitrogen dioxide, could therefore be higher on low ozone days, acting as a competing risk in this association and potentially driving a negative interaction in some ZCTAs. Additionally, the perceived risk of air pollution and high heat events may alter behaviors and decrease exposure when there is a dual threat of ozone and heat exposure (63); this may vary based on the capacity of populations to adapt, which may be related to resource and socioeconomic factors.

As shown in the metaregression results, neighborhood-level environmental characteristics modify the vulnerability of specific ZCTAs to ozone and heat joint exposures. Previous research has shown that high settlement density and sparse vegetation can increase the human thermal comfort index, an indicator of heat stress (64). In our results, population density was found to have a slight positive association with ozone–heat interactive effects, but this estimate was not precise (Fig. 4). Tree canopy, a measure of green space at the ZCTA level, was not found to be a strong predictor of joint effects either, although it did have a slight protective effect (Fig. 4). Although the interaction hotspots we observe are not consistently concentrated in the highly urbanized areas of California, the total population showed a strong positive association with observed interactive effects in the metaregression results. This heterogeneity may be explained by neighborhood-level demographic differences within highly urbanized areas.

Minority populations and those of a low socioeconomic status are particularly vulnerable to heat (32) and ozone (65) due to the range of associated individual- and neighborhood-level factors that increase risk in these specific populations. Racial microaggressions and racism experienced by individuals from minority groups may also hinder their comfort in seeking care (66). Our results are consistent with this finding, as zip codes with a higher proportion of non-White populations showed a stronger joint effect of ozone and heat (Fig. 4). Interestingly, such an effect is no longer observed after adjusting for median income (*SI Appendix*, Table S4). As discussed recently, race/ethnicity (both for individual-level self-reported race/ethnicity or neighborhood race/ethnicity composition) in environmental epidemiological studies operates through various pathways such as differential socioeconomic status to generate observed environmental health disparities of interest (67). As described in the social epidemiological literature (68), such patterns can be interpreted as mediated inequality measures, which correspond to what would happen to race/ethnic inequalities for a given health outcome if certain socioeconomic status (like income) distributions were set to something other than what they in fact were across racial/ethnic subgroups. In the context of our findings, it means that if we were able to (hypothetically) reduce income inequalities between race/ethnic groups (at the neighborhood level) to zero, observed race/ethnic disparities regarding the joint impacts of extreme heat and ozone would disappear. Interestingly, such patterns have been found in other studies in environmental epidemiology (67) or in the context of COVID-19 test positivity and risk of hospitalization (69).

That being said, the positive association between median income and the role of the proportion of unemployed residents in driving joint effects also exemplifies differential susceptibility to environmental determinants and demonstrates the strong role of neighborhood socioeconomic status in driving this increased vulnerability to joint effects of heat and ozone exposure. Exposure to multiple environmental risks, such as other toxins and poor housing quality (70), as well as social deprivation from lack of access to proper healthcare and education can increase the vulnerability of populations from a lower socioeconomic status (71). Older populations are considered to be more vulnerable to both heat (72) and ozone exposures (73), although our results do not indicate that zip codes with a higher elderly population have increased vulnerability. Our results can be used to prioritize specific neighborhoods that are considered at a higher risk for joint ozone–heat effects, such as those with lower income and with a higher rate of unemployment.

Certain commuting and travel behaviors can also play a role in the joint health effects of ozone and extreme heat events. In our results, the percentage of workers commuting by walking, cycling, or transit was shown to be associated with decreased joint effects, and automobile ownership showed the opposite, indicating that car usage may a predictor of joint effects. Reduced car travel has been shown to have health benefits through reduced air pollution exposure and increased exercise (74). Specifically, using bicycles for urban travel has been found to drive health benefits from decreased emissions (75). Increased walking and bicycling in California have been shown to contribute to disease reduction (76). However, accessibility to walking and bicycling for commuting is also strongly correlated with neighborhood socioeconomic status (77), which is partially driving the association we observe. Although a higher percentage of workers commuting by walking, cycling, or transit remains associated with decreased joint effects after adjusting for income (*SI Appendix*, Table S4), there may be various other factors related to the socioeconomic context of the ZCTA that may explain this association.

Lastly, long-term exposure to other air pollutants were found to be associated with increased joint effects, indicating that there may be multipollutant effects. This may be related to environmental injustices, as low-income areas and communities of color have a disproportionate exposure to air pollutant concentrations (78). The Central Valley, where we observe a large hotspot of strong interactive effects, has some of the worst air quality in the nation; this has been shown to be associated with the highest rates of asthma in California (79). These findings indicate the importance of considering neighborhood-level characteristics in understanding the vulnerability of specific areas to interactive ozone and heat effects.

Our results demonstrate the importance of going beyond an overall regional measure to consider fine spatial heterogeneity in the effects and thresholds for early warning systems. Without considering these effects at a local scale, positive associations may be concealed. In the future, it would be important to assess the spatial variation in effects in other studies which found limited or no joint effects of ozone and heat in other regions. Additionally, this methodology can be applied to other exposures to understand their spatial heterogeneity and identify susceptible areas that can be used to inform targeted interventions.

There are a few limitations to this study that should be acknowledged. Missing values for ozone left some gaps in our

understanding in certain areas of California (23.4% of zip codes do not have ozone information; missing data shown in *SI Appendix*, Fig. S9); zero values for hospital visits also led to some difficulties in examining this association at the ZCTA level. Existing methodologies for the use of spatial effects do not allow for anisotropy in spatial processes. The assumption of isotropy does not hold for data across complex geographies of regions and climates such as that of California, where, for example, heat wave expressions at the highly populated coast are modulated by coastal marine-layer clouds (80). There is room for methodological development in this area, and we plan to explore more flexible methodologies. Lastly, heat waves are expected to become more humid in California (5); understanding the role of humidity in driving ozone and heat interaction is an important area for future work.

Climate change projections show that the frequency, intensity, and duration of extreme heat events as well as days of high ozone concentration are expected to increase (5, 6, 39). This study helps understand predictors in the spatial distribution of these effects and can be used to inform and target joint early warning systems to protect populations from the deleterious effects of both ozone and heat.

Data Availability. The code and simulated sample dataset for reproducibility purposes is provided at the following link: https://github.com/benmarhnia-lab/JointOzoneHeatWaves.

ACKNOWLEDGMENTS. This work was supported by the Office of Environmental Health Hazard Assessment No. 18-E0012.

1. F. J. Kelly, G. W. Fuller, H. A. Walton, J. C. Fussell, Monitoring air pollution: Use of early warning systems for public health. *Respirology* **17**, 7–19 (2012).
2. J. Wang, X. Zhang, Z. Guo, H. Lu, Developing an early-warning system for air quality prediction and assessment of cities in China. *Expert Syst. Appl.* **84**, 102–116 (2017).
3. G. Toloo, G. FitzGerald, P. Aitken, K. Verrall, S. Tong, Evaluating the effectiveness of heat warning systems: Systematic review of epidemiological evidence. *Int. J. Public Health* **58**, 667–681 (2013).
4. D. Lowe, K. L. Ebi, B. Forsberg, Heatwave early warning systems and adaptation advice to reduce human health consequences of heatwaves. *Int. J. Environ. Res. Public Health* **8**, 4623–4648 (2011).
5. A. Gershunov, K. Guirguis, California heat waves in the present and future. *Geophys. Res. Lett.* **39**, 18710 (2012).
6. A. Mahmud, M. Tyree, D. Cayan, N. Motallebi, M. J. Kleeman, Statistical downscaling of climate change impacts on ozone concentrations in California. *J. Geophys. Res. D Atmospheres* **113**, 10.1029/2007JD009534 (2008).
7. J. L. Schnell, M. J. Prather, Co-occurrence of extremes in surface ozone, particulate matter, and temperature over eastern North America. *Proc. Natl. Acad. Sci. U.S.A.* **114**, 2854–2859 (2017).
8. D. Phung *et al*., Ambient temperature and risk of cardiovascular hospitalization: An updated systematic review and meta-analysis. *Sci. Total Environ.* **550**, 1084–1102 (2016).
9. Z. Xu, G. FitzGerald, Y. Guo, B. Jalaludin, S. Tong, Impact of heatwave on mortality under different heatwave definitions: A systematic review and meta-analysis. *Environ. Int.* **89-90**, 193–203 (2016).
10. A. Bouchama *et al*., A model of exposure to extreme environmental heat uncovers the human transcriptome to heat stress. *Sci. Rep.* **7**, 9429 (2017).
11. P. Michelozzi *et al*.; PHEWE Collaborative Group, High temperature and hospitalizations for cardiovascular and respiratory causes in 12 European cities. *Am. J. Respir. Crit. Care Med.* **179**, 383–389 (2009).
12. R. S. Green *et al*., The effect of temperature on hospital admissions in nine California counties. *Int. J. Public Health* **55**, 113–121 (2010).
13. G. B. Anderson *et al*., Heat-related emergency hospitalizations for respiratory diseases in the Medicare population. *Am. J. Respir. Crit. Care Med.* **187**, 1098–1103 (2013).
14. C. J. Gronlund, A. Zanobetti, J. D. Schwartz, G. A. Wellenius, M. S. O'Neill, Heat, heat waves, and hospital admissions among the elderly in the United States, 1992-2006. *Environ. Health Perspect.* **122**, 1187–1192 (2014).
15. D. Nuvolone, D. Petri, F. Voller, The effects of ozone on human health. *Environ. Sci. Pollut. Res. Int.* **25**, 8074–8088 (2018).
16. S. Magzamen, B. F. Moore, M. G. Yost, R. A. Fenske, C. J. Karr, Ozone-related respiratory morbidity in a low-pollution region. *J. Occup. Environ. Med.* **59**, 624–630 (2017).
17. B. J. Malig *et al*., A time-stratified case-crossover study of ambient ozone exposure and emergency department visits for specific respiratory diagnoses in California (2005–2008). *Environ. Health Perspect.* **124**, 745–753 (2016).
18. H. Liu *et al*., Ground-level ozone pollution and its health impacts in China. *Atmos. Environ.* **173**, 223–230 (2018).
19. M. H. Forouzanfar *et al*.; GBD 2015 Risk Factors Collaborators, Global, regional, and national comparative risk assessment of 79 behavioural, environmental and occupational, and metabolic risks or clusters of risks, 1990-2015: A systematic analysis for the global burden of disease study 2015. *Lancet* **388**, 1659–1724 (2016).
20. L. Filleul *et al*., The relation between temperature, ozone, and mortality in nine French cities during the heat wave of 2003. *Environ. Health Perspect.* **114**, 1344–1347 (2006).
21. R. W. Atkinson *et al*., Long-term exposure to ambient ozone and mortality: A quantitative systematic review and meta-analysis of evidence from cohort studies. *BMJ Open* **6**, e009493 (2016).
22. J. Madrigano, D. Jack, G. B. Anderson, M. L. Bell, P. L. Kinney, Temperature, ozone, and mortality in urban and non-urban counties in the northeastern United States. *Environ. Health* **14**, 3 (2015).
23. P. H. Fischer, B. Brunekreef, E. Lebret, Air pollution related deaths during the 2003 heat wave in The Netherlands. *Atmos. Environ.* **38**, 1083–1085 (2004).
24. S. Tong, C. Ren, N. Becker, Excess deaths during the 2004 heatwave in Brisbane, Australia. *Int. J. Biometeorol.* **54**, 393–400 (2010).
25. C. Ren, G. M. Williams, K. Mengersen, L. Morawska, S. Tong, Does temperature modify short-term effects of ozone on total mortality in 60 large eastern US communities? An assessment using the NMMAPS data. *Environ. Int.* **34**, 451–458 (2008).
26. W. Shi *et al*., Modification effects of temperature on the ozone-mortality relationship: A nationwide multicounty study in China. *Environ. Sci. Technol.* **54**, 2859–2868 (2020).
27. S. Pattenden *et al*., Ozone, heat and mortality: Acute effects in 15 British conurbations. *Occup. Environ. Med.* **67**, 699–707 (2010).
28. M. Scortichini *et al*., Short-term effects of heat on mortality and effect modification by air pollution in 25 Italian cities. *Int. J. Environ. Res. Public Health* **15**, 1771 (2018).
29. I. Jhun, N. Fann, A. Zanobetti, B. Hubbell, Effect modification of ozone-related mortality risks by temperature in 97 US cities. *Environ. Int.* **73**, 128–134 (2014).
30. A. Wilson, A. G. Rappold, L. M. Neas, B. J. Reich, Modeling the effect of temperature on ozone-related mortality. *Ann. Appl. Stat.* **8**, 1728–1749 (2014).
31. A. D. Hackbarth, J. A. Romley, D. P. Goldman, Racial and ethnic disparities in hospital care resulting from air pollution in excess of federal standards. *Soc. Sci. Med.* **73**, 1163–1168 (2011).
32. C. J. Gronlund, Racial and socioeconomic disparities in heat-related health effects and their mechanisms: A review. *Curr. Epidemiol. Rep.* **1**, 165–173 (2014).
33. A. Analitis *et al*., Effects of heat waves on mortality: Effect modification and confounding by air pollutants. *Epidemiology* **25**, 15–22 (2014).
34. J. Li *et al*., Modification of the effects of air pollutants on mortality by temperature: A systematic review and meta-analysis. *Sci. Total Environ.* **575**, 1556–1570 (2017).
35. K. J. Rothman, S. Greenland, A. M. Walker, Concepts of interaction. *Am. J. Epidemiol.* **112**, 467–470 (1980).
36. T. J. VanderWeele, M. J. Knol, A tutorial on interaction. *Epidemiol. Methods* **3**, 33–72 (2014).
37. Cal-Adapt, Exploring California's climate change research. https://cal-adapt.org/data/. Accessed 1 June 2018.
38. B. Livneh *et al*., A spatially comprehensive, hydrometeorological data set for Mexico, the U.S., and Southern Canada 1950-2013. *Sci. Data* **2**, 150042 (2015).
39. A. Gershunov, D. R. Cayan, S. F. Iacobellis, The great 2006 heat wave over California and Nevada: Signal of an increasing trend. *J. Clim.* **22**, 6181–6203 (2009).
40. EPA, Air quality system. https://www.epa.gov/aqs. Accessed 1 June 2018.
41. EPA, 2015 National ambient air quality standards (NAAQS) for ozone. (2018). (https://www.epa.gov/ground-level-ozone-pollution/2015-national-ambient-air-quality-standards-naaqs-ozone). Accessed 1 June 2018.
42. R. Basu, B. D. Ostro, A multicounty analysis identifying the populations vulnerable to mortality associated with high ambient temperature in California. *Am. J. Epidemiol.* **168**, 632–637 (2008).
43. R. Basu, W.-Y. Feng, B. D. Ostro, Characterizing temperature and mortality in nine California counties. *Epidemiology* **19**, 138–145 (2008).
44. S. Tong, X. Y. Wang, Y. Guo, Assessing the short-term effects of heatwaves on mortality and morbidity in Brisbane, Australia: Comparison of case-crossover and time series analyses. *PloS One* **7**, e37500 (2012).
45. D. B. Richardson, J. S. Kaufman, Estimation of the relative excess risk due to interaction and associated confidence bounds. *Am. J. Epidemiol.* **169**, 756–760 (2009).
46. D. W. Hosmer, S. Lemeshow, Confidence interval estimation of interaction. *Epidemiology* **3**, 452–456 (1992).
47. R. Aguilera *et al*., Respiratory hospitalizations and wildfire smoke: A spatiotemporal analysis of an extreme firestorm in San Diego County, California. *Environ. Epidemiol.* **4**, e114 (2020).
48. A. O. Finley, S. Banerjee, B. P. Carlin, spBayes: An R package for univariate and multivariate hierarchical point-referenced spatial models. *J. Stat. Softw.* **19**, 1–24 (2007).
49. Anonymous, U.S. Census Bureau. American Community Survey (2010). Retrieved from https://www.census.gov/programs-surveys/acs. Accessed 20 May 2020.
50. M. Marmor, Heat wave mortality in New York City, 1949 to 1970. *Arch. Environ. Health* **30**, 130–136 (1975).
51. H. Gong Jr, M. S. McManus, W. S. Linn, Attenuated response to repeated daily ozone exposures in asthmatic subjects. *Arch. Environ. Health* **52**, 34–41 (1997).
52. T. Delaney *et al*., "Healthy places index" (Public Health Alliance of Southern California, Long Beach, CA, 2018).

53. NWS, NWS experimental heatrisk: Identifying potential heat risks in the seven day forecast. HeatRisk (2019). https://www.wrh.noaa.gov/wrh/heatrisk/?wfo=sgx. Accessed 1 June 2019.
54. T. Benmarhnia, L. Schwarz, A. Nori-Sarma, M. L. Bell, Quantifying the impact of changing the threshold of New York City Heat Emergency Plan in reducing heat-related illnesses. *Environ. Res. Lett.* **14**, 114006 (2019).
55. T. Benmarhnia *et al*., A difference-in-differences approach to assess the effect of a heat action plan on heat-related mortality, and differences in effectiveness according to sex, age, and socioeconomic status (Montreal, Quebec). *Environ. Health Perspect.* **124**, 1694–1699 (2016).
56. Z. Qian *et al*., High temperatures enhanced acute mortality effects of ambient particle pollution in the "oven" city of Wuhan, China. *Environ. Health Perspect.* **116**, 1172–1178 (2008).
57. M. Pascal *et al*., Ozone and short-term mortality in nine French cities: Influence of temperature and season. *Atmos. Environ.* **62**, 566–572 (2012).
58. C.-M. Lin, C.-M. Liao, Temperature-dependent association between mortality rate and carbon monoxide level in a subtropical city: Kaohsiung, Taiwan. *Int. J. Environ. Health Res.* **19**, 163–174 (2009).
59. C. Ren, G. M. Williams, K. Mengersen, L. Morawska, S. Tong, Temperature enhanced effects of ozone on cardiovascular mortality in 95 large US communities, 1987-2000: Assessment using the NMMAPS data. *Arch. Environ. Occup. Health* **64**, 177–184 (2009).
60. R. Basu, D. Pearson, B. Malig, R. Broadwin, R. Green, The effect of high ambient temperature on emergency room visits. *Epidemiology* **23**, 813–820 (2012).
61. K. Guirguis, A. Gershunov, A. Tardy, R. Basu, The impact of recent heat waves on human health in California. *J. Appl. Meteorol. Climatol.* **53**, 3–19 (2014).
62. I. Jhun, B. A. Coull, A. Zanobetti, P. Koutrakis, The impact of nitrogen oxides concentration decreases on ozone trends in the USA. *Air Qual. Atmos. Health* **8**, 283–292 (2015).
63. J. C. Semenza *et al*., Public perception and behavior change in relationship to hot weather and air pollution. *Environ. Res.* **107**, 401–411 (2008).
64. S. L. Harlan, A. J. Brazel, L. Prashad, W. L. Stefanov, L. Larsen, Neighborhood microclimates and vulnerability to heat stress. *Soc. Sci. Med.* **63**, 2847–2863 (2006).
65. M. L. Bell, A. Zanobetti, F. Dominici, Who is more affected by ozone pollution? A systematic review and meta-analysis. *Am. J. Epidemiol.* **180**, 15–28 (2014).
66. K. Babla *et al*., Racial microaggressions within respiratory and critical care medicine. *Lancet Respir. Med.* **9**, e27–e28 (2021).
67. T. Benmarhnia, A. Hajat, J. S. Kaufman, Inferential challenges when assessing racial/ethnic health disparities in environmental research. *Environ. Health* **20**, 7 (2021).
68. T. J. VanderWeele, W. R. Robinson, On the causal interpretation of race in regressions adjusting for confounding and mediating variables. *Epidemiology* **25**, 473–484 (2014).
69. H. B. Gershengorn *et al*.; UHealth-DART Research Group, Association of race and ethnicity with COVID-19 test positivity and hospitalization is mediated by socioeconomic factors. *Ann. Am. Thorac. Soc.*, 10.1513/AnnalsATS.202011-1448OC (2021).
70. G. W. Evans, E. Kantrowitz, Socioeconomic status and health: The potential role of environmental risk exposure. *Annu. Rev. Public Health* **23**, 303–331 (2002).
71. J. Schnittker, Education and the changing shape of the income gradient in health. *J. Health Soc. Behav.* **45**, 286–305 (2004).
72. T. Benmarhnia, S. Deguen, J. S. Kaufman, A. Smargiassi, Vulnerability to heat-related mortality. *Epidemiology* **26**, 781–793 (2015).
73. M. Medina-Ramón, J. Schwartz, Who is more vulnerable to die from ozone air pollution? *Epidemiology* **19**, 672–679 (2008).
74. M. L. Grabow *et al*., Air quality and exercise-related health benefits from reduced car travel in the midwestern United States. *Environ. Health Perspect.* **120**, 68–76 (2012).
75. G. Lindsay, A. Macmillan, A. Woodward, Moving urban trips from cars to bicycles: Impact on health and emissions. *Aust. N. Z. J. Public Health* **35**, 54–60 (2011).
76. N. Maizlish, N. J. Linesch, J. Woodcock, Health and greenhouse gas mitigation benefits of ambitious expansion of cycling, walking, and transit in California. *J. Transp. Health* **6**, 490–500 (2017).
77. S. Zahran, S. D. Brody, P. Maghelal, A. Prelog, M. Lacy, Cycling and walking: Explaining the spatial distribution of healthy modes of transportation in the United States. *Transp. Res. Part D Transp. Environ.* **13**, 462–470 (2008).
78. J. G. Su *et al*., An index for assessing demographic inequalities in cumulative environmental hazards with application to Los Angeles. *Environ. Sci. Technol.* **43**, 7626–7634 (2009).
79. Y.-Y. Meng *et al*., Outdoor air pollution and uncontrolled asthma in the San Joaquin Valley, California. *J. Epidemiol. Community Health* **64**, 142–147 (2010).
80. R. E. Clemesha, K. Guirguis, A. Gershunov, I. J. Small, A. Tardy, California heat waves: Their spatial evolution, variation, and coastal modulation by low clouds. *Clim. Dyn.* **50**, 4285–4301 (2018).